Enhancement of resonant structure in the photoelectron spectra of excited He($2\,^1S^e$) above the $n=2$ threshold

I. Sánchez and F. Martín
Departamento de Química, Facultad de Ciencias, C-14, Universidad Autónoma de Madrid, 28049-Madrid, Spain
(Received 27 July 1992)

We have calculated partial cross sections for photoionization of helium in the $2\,^1S^e$ metastable state above the $n=2$ threshold. In this process, most of the He^+ ions remain in an $n=2$ excited state so that interactions involving the degenerate $n=2$ open channels can be more easily studied. Our results show that an enhancement of the resonance structures is observed in both total and $n=2$ partial cross sections with respect to ground-state photoionization. The origin of this effect is discussed in detail.

PACS number(s): 32.80.Fb, 32.80.Dz, 31.50.+w

The photoelectron spectra of He between the $n=2$ and 3 thresholds is the result of a complicated pattern of interactions and interferences between different open channels and $3lnl'$ doubly excited (resonant) states, in which electron correlation plays a crucial role. Most of the autoionization of the $3lnl'$ doubly excited states goes through the $n=2$ channels ($2s\varepsilon p$, $2p\varepsilon s$, and $2p\varepsilon d$), and therefore, the largest continuum-resonance interferences are found by measuring the corresponding $n=2$ partial photoionization cross sections. In this respect, a number of experimental groups have been able to provide photoionization cross sections for He($1s^2$, $1\,^1S^e$) leaving the He^+ ion in a $2s$ and/or a $2p$ excited state [1]. Unfortunately, when helium is in the $1\,^1S^e$ ground state, almost 90% of the photoionization occurs in the $1s\varepsilon p$ channel, where the resonance structure is less apparent. This implies that the experimental determination of the $n=2$ cross sections is not easy and that an enhancement of these cross sections as well as of the associated resonance structure would be desirable.

In this work we consider photoionization of He from the excited $2\,^1S^e$ bound state. The reasons for choosing such a state are (i) the initial angular momentum, spin, and parity are the same as for the ground state; (ii) the continuum states and, in particular, the resonances exhibited in the corresponding photoelectron spectra are, as for ground-state photoionization, of $^1P^o$ symmetry; (iii) photoionization to the $2s\varepsilon p$ channel is the dominant process; and (iv) the $2\,^1S^e$ state is metastable, i.e., its lifetime, $\tau \simeq 2\times 10^{-2}$ sec [2], should be long enough to carry out a photoionization experiment from such a state. Points (i) and (ii) ensure that photoionization from the ground and metastable $2\,^1S^e$ states can be easily compared; and point (iii), that the interference between nonresonant and resonant (autoionizing) processes will be more clearly displayed.

Previous theoretical works for the photoionization of metastable He($2\,^1S^e$) have reported resonance parameters below the $n=2$ threshold where a single $1s\varepsilon p$ channel is open [3–5]. Above this threshold, we are only aware of the papers of Jacobs and Burke [6], and Bell, Kingston, and Taylor [7], who did not include resonance structure. Wague [8] has partially tackled this aspect and provided line-profile parameters for a few resonances. The purpose of this paper is to perform a complete study of the photoionization of He($2\,^1S^e$) between the $n=2$ and 3 thresholds including the whole resonance structure, and to analyze the influence of the initial-state correlation in the photoionization cross sections. The theoretical method used in this work is the same as we proposed to study photoionization of helium from the ground state [9] (hereafter called paper I).

The $2\,^1S^e$ state has been obtained in a configuration-interaction (CI) calculation performed with a basis of 130 configurations built from optimized Slater-type orbitals (STO's). The resulting wave function satisfies the virial theorem with an accuracy of 10^{-5} a.u., and the corresponding energy is $-2.145\,90$ a.u., to be compared with $-2.145\,97$ a.u., which is the accurate nonrelativistic value calculated by Pekeris [10].

The exact final-state wave function for each channel μ can be written as [9]

$$|\psi^-_{\mu E}\rangle = \frac{\langle \phi_s|QHP|P\psi^{0-}_{\mu E}\rangle}{E-\mathcal{E}_s-\Delta_s(E)-i\dfrac{\Gamma_s(E)}{2}}|\phi_s\rangle + [1+G^{(s)}_Q(E)QHP]\left[|P\psi^{0-}_{\mu E}\rangle + \frac{\langle \phi_s|QHP|P\psi^{0-}_{\mu E}\rangle}{E-\mathcal{E}_s-\Delta_s(E)-i\dfrac{\Gamma_s(E)}{2}} G^{(s)-}_P(E)PHQ|\phi_s\rangle\right], \quad (1)$$

where P and Q are the usual projection operators of the Feshbach-O'Malley formalism [11,12], the resonances ϕ_n are eigenfunctions of QHQ with eigenvalues $\mathcal{E}_n$, $G^{(s)}_Q(E)$ is the Q-subspace Green operator from which the ϕ_s resonance has been excluded, the nonresonant states $P\psi^{0-}_{\mu E}$ are eigenfunctions of $PHP+PHQG^{(s)}_Q(E)QHP$ with eigenvalues E, $G^{(s)-}_P(E)$ is the corresponding Green operator with incoming behavior, $\Gamma_s(E)$ is the energy-

dependent "total width" of the ϕ_s resonance, and $\Delta_s(E)$ is its energy-dependent "shift."

The resonant ϕ_n and nonresonant continuum $P\psi^{0-}_{\mu E}$ states are those already used in paper I. The former have been obtained with the pseudopotential Feshbach method [12] in a representation of 208 configurations built from STO's which accurately reproduces the $3lnl'\ ^1P^o$ doubly excited states. The latter have been calculated by solving iteratively the scattering K-matrix equations [9] for a given energy E in a representation of discretized uncoupled continuum states. The resulting $P\psi^{0-}_{\mu E}$ wave functions are then correctly δ normalized, fully include interchannel coupling, and satisfy the correct asymptotic conditions. The operator $G^{(s)-}_P$ is evaluated with an algebraic Green-function expansion which provides each term from the preceding one without calculating additional matrix elements (see paper I). $G^{(s)}_Q$ is built from the 48 lowest eigenfunctions of $Q\mathcal{H}Q$, i.e., it includes the $3l\varepsilon l'$ continuum channels as well as all the $3lnl'$ and $4lnl'$ doubly excited states that our STO basis is able to reproduce.

We have performed calculations in the energy range $E=47.5-51.9$ eV, using an energy grid with variable step size in order to make explicit all the resonant structures. The photoionization cross sections have been evaluated in the dipole approximation. We have shown [13] that the bases used for the resonant and nonresonant wave functions are large enough to ensure almost invariant results in both the length and velocity gauges. Therefore, in this paper we will only present results obtained in the length representation.

Our calculated $1s\varepsilon p$, $2s\varepsilon p$, $2p\varepsilon s$, and $2p\varepsilon d$ partial cross sections are shown in Fig. 1, and those for the total cross section are shown in Fig. 2. As is apparent from Fig. 1, the background associated to the $2s\varepsilon p$ partial cross section is the largest one (notice the different scales used in Fig. 1). This cannot be attributed to correlation, as can be easily understood by using a simple hydrogenic model. (From now on we will use the subscripts g and m for all the quantities referred to ground-state photoionization and metastable $2\ ^1S^e$ photoionization, respectively.) Assuming that the initial state ψ_m is described by a single hydrogenic configuration $1s2s$, and the final state by a hydrogenic orbital and a Coulomb wave function, we get

$$\begin{aligned}
&\langle\psi_m|z_1+z_2|\psi_{1s\varepsilon p}\rangle=2\langle 2s|z|\varepsilon p\rangle\ ,\\
&\langle\psi_m|z_1+z_2|\psi_{2s\varepsilon p}\rangle=2\langle 1s|z|\varepsilon p\rangle\ ,\\
&\langle\psi_m|z_1+z_2|\psi_{2p\varepsilon s}\rangle=\langle\psi_m|z_1+z_2|\psi_{2p\varepsilon d}\rangle=0\ ,
\end{aligned}\tag{2}$$

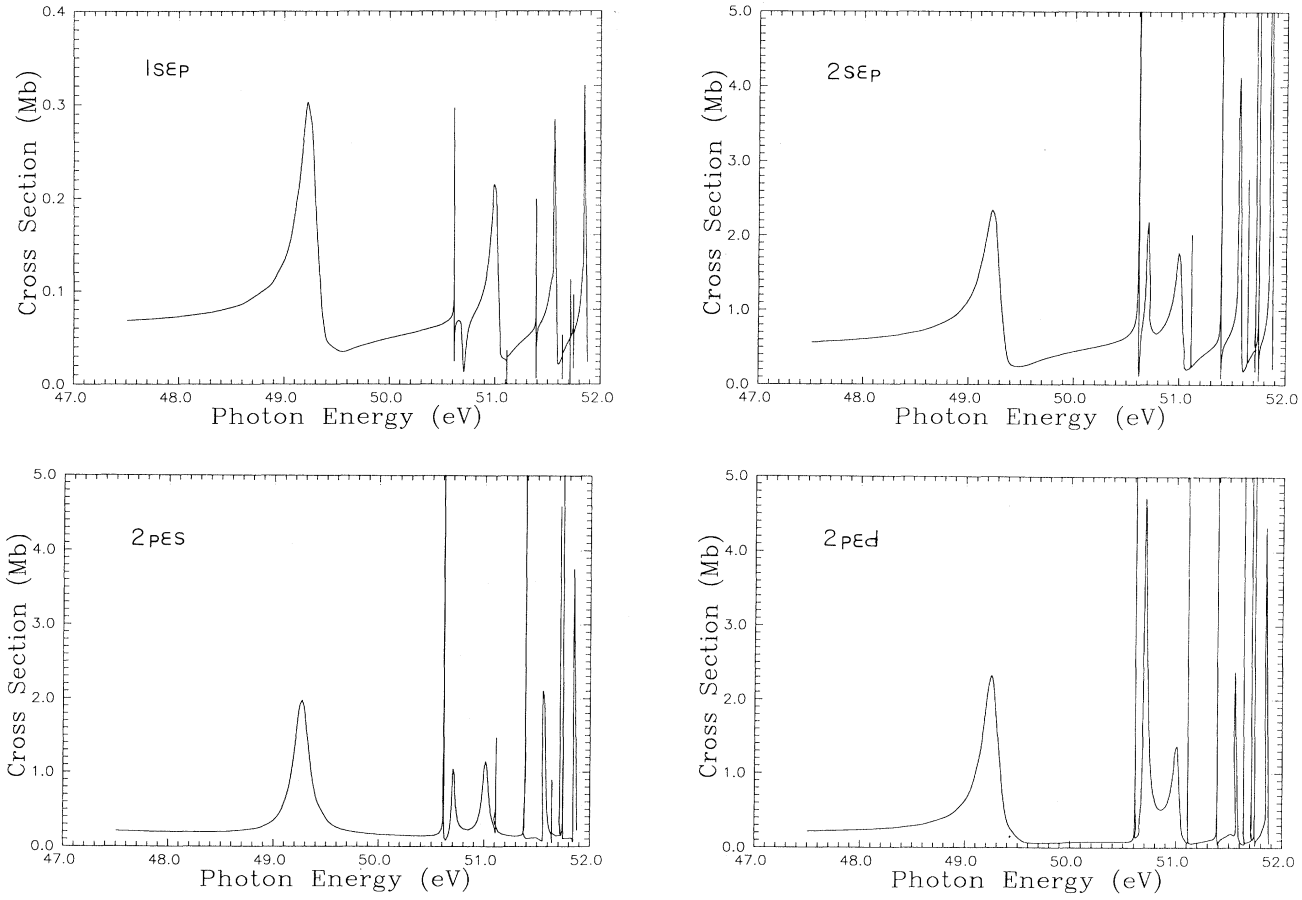

FIG. 1. Partial photoionization cross sections of He($2\ ^1S^e$).

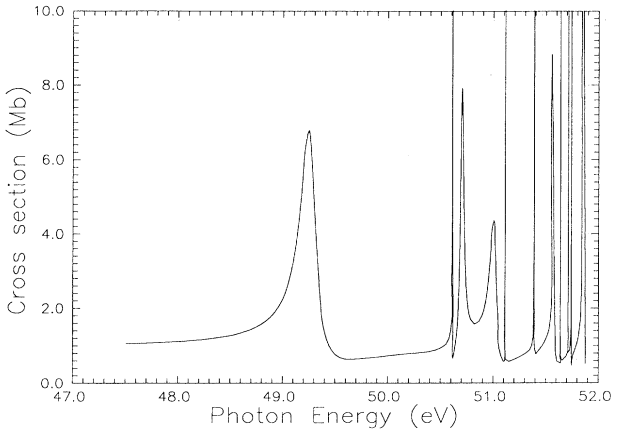

FIG. 2. Total photoionization cross section of He(2 $^1S^e$).

which explains the fact that the $2s\varepsilon p$ cross section is predominant. This is in contrast with photoionization from the ground state, where

$$\begin{aligned}\langle\psi_g|z_1+z_2|\psi_{1s\varepsilon p}\rangle &= 2\langle 1s|z|\varepsilon p\rangle\ ,\\ \langle\psi_g|z_1+z_2|\psi_{2s\varepsilon p}\rangle &= \langle\psi_g|z_1+z_2|\psi_{2p\varepsilon s}\rangle\\ &= \langle\psi_g|z_1+z_2|\psi_{2p\varepsilon d}\rangle = 0\ ,\end{aligned} \tag{3}$$

and, therefore, photoionization mainly occurs in the $1s\varepsilon p$ channel [1]. These simple ideas also explain why the $2s\varepsilon p+2p\varepsilon s+2p\varepsilon d$ background in the first case is roughly of the same order as the $1s\varepsilon p$ one in the second.

Another important consequence that can be extracted from Figs. 1 and 2 is that the resonance structures in the $2s\varepsilon p$, $2p\varepsilon s$, and $2p\varepsilon d$ partial cross sections, and especially in the total cross section, are much more pronounced than for photoionization from the ground state [9]. In particular, the values of the cross sections at the maxima are larger (for needlelike resonances, they can reach 100 Mb). Also, the peaks present a shape that is closer to a Lorentzian profile than to a typical interfering Fano profile. To explain these findings, we have evaluated the Fano parameters [14] that permit us to fit the total cross section to the usual formula:

$$\sigma_m(E)=\sigma_m^0(E)\left[\rho_m^2\frac{(q_m+\epsilon)^2}{1+\epsilon^2}+1-\rho_m^2\right]\ , \tag{4}$$

in the vicinity of each resonance. In Eq. (4), $\sigma_m^0(E)$ is the background nonresonant cross section, $\epsilon=2[E-\mathcal{E}_s-\Delta_s(E)]/\Gamma_s(E)$, q_m is the line-profile parameter, and ρ_m^2 is the so-called correlation parameter. As explained in paper I, σ^0, ρ^2, and q come out directly from our calculations and no real fitting is needed to obtain them. Our equations for σ^0, ρ^2, and q take into account the effect of neighboring resonances through the terms including the $G_Q^{(s)}$ operator and, therefore, slightly differ from those proposed by Fano [14]. In Table I we present the set of parameters E_s, Γ_s, σ_m^0, ρ_m^2, and q_m for the first 10 resonances. We have also included ρ_g^2 and q_g for photoionization from the ground state (taken from paper I), and the (K,T) quantum numbers introduced by Herrick and Sinanoglu [15], which are useful to classify approximately doubly excited states with similar correlation properties [in some cases such a labeling must be taken with caution due to a strong mixing between different series of (K,T) states]. In order to simplify the discussion that follows, let us write q and ρ^2 in the single-isolated-resonance approximation [14]:

$$q_m=\frac{\langle\psi_m|z_1+z_2|\phi_s\rangle+\mathrm{Re}[\langle\psi_m|z_1+z_2|G_P^{(s)-}(\mathcal{E}_s)P\mathcal{H}Q\phi_s\rangle]}{\pi\sum_\nu\langle\psi_m|z_1+z_2|P\psi^{0-}_{\nu\mathcal{E}_s}\rangle\langle P\psi^{0-}_{\nu\mathcal{E}_s}|P\mathcal{H}Q|\phi_s\rangle}\ , \tag{5}$$

$$\rho_m^2=\frac{\left[\sum_\nu\langle\psi_m|z_1+z_2|P\psi^{0-}_{\nu\mathcal{E}_s}\rangle\langle P\psi^{0-}_{\nu\mathcal{E}_s}|P\mathcal{H}Q|\phi_s\rangle\right]^2}{\frac{\Gamma_s(\mathcal{E}_s)}{2\pi}\sum_\nu|\langle\psi_m|z_1+z_2|P\psi^{0-}_{\nu\mathcal{E}_s}\rangle|^2}\ . \tag{6}$$

The values for q are entirely due to correlation, since a single-hydrogenic-configuration description of the states involved in Eq. (6) would yield $q_g=q_m=0$. It can be observed that q_m values belonging to a particular (K,T) series, i.e., states with similar correlation properties, are roughly comparable [for instance, $q_m=-4.6$, -3.1, -3.5 for the $(1,1)_n$ states]. This behavior is less apparent for ρ^2 since this parameter is bounded between 0

TABLE I. Fano parameters for the first ten resonances observed in the total photoionization cross section of He(2 $^1S^e$). q_g and ρ_g^2 correspond to photoionization of helium in the ground state.

$(K,T)_n$	E_s (eV)	Γ_s (eV)	σ_m^0 (Mb)	ρ_m^2	ρ_g^2	q_m	q_g
$(1,1)_3$	49.2719	0.174 3	0.9291	0.2974	0.050 3	−4.610	1.300
$(2,0)_4$	50.6144	0.000 8	1.0463	0.5424	0.000 05	−14.945	−17.852
$(-1,1)_3$	50.7058	0.035 5	0.9743	0.0427	0.033 6	12.894	−0.0362
$(1,1)_4$	51.0134	0.070 4	0.8987	0.4039	0.044 0	−3.109	1.508
$(0,0)_4$	51.1135	0.000 5	0.5524	0.0105	0.012 4	42.904	0.557
$(2,0)_5$	51.3892	0.000 5	0.8572	0.5195	0.000 2	−13.699	−10.590
$(-1,1)_4$	51.5507	0.014 0	2.9287	0.2840	0.012 7	2.061	0.782
$(1,1)_5$	51.5657	0.027 4	0.9489	0.4722	0.046 7	−3.541	1.399
$(0,0)_5$	51.6403	0.000 2	0.5524	0.0581	0.004 9	18.499	0.935
$(-2,0)_4$	51.7152	0.000 01	0.7894	0.0062	0.009 0	76.199	−1.148

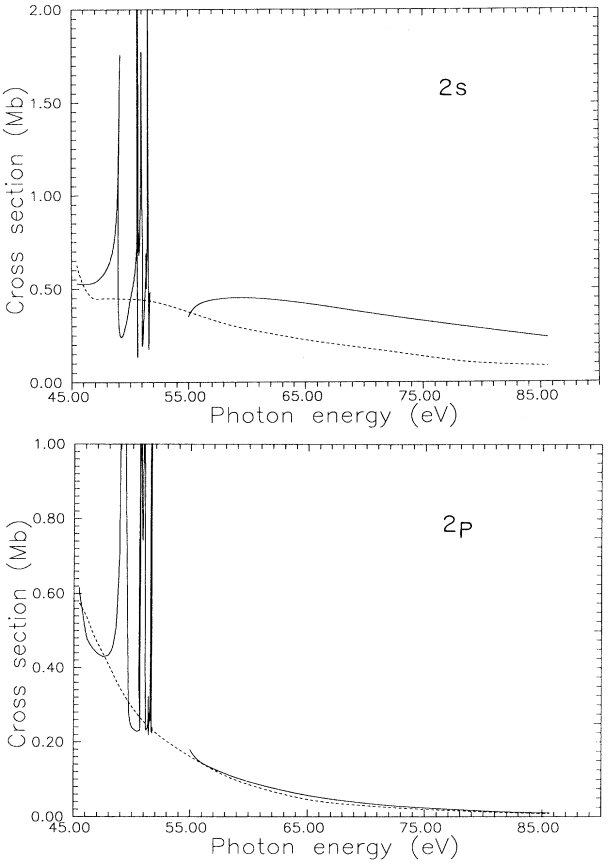

FIG. 3. $2s$ and $2p$ partial photoionization cross section of He($2\,{}^1S^e$) up to 85 eV; ——, our results; — — —, Jacobs and Burke [6].

and 1. Inspection of Table I shows that q depends strongly on the initial state used to perform photoionization. Also, whereas there is a sign inversion for the $(1,1)_n$ series, this is not the case for the $(2,0)_n$ one. This is in contrast with Wague's conclusion [8] on a systematic sign inversion for all resonances, since their q_g values strongly disagree with ours. The origin of this discrepancy is probably the neglect of inter-channel coupling and the reduced size of the basis set in Wague's calculations.

In Table I we can observe that $|q_m| > |q_g|$ in most cases. This is so because the first term in the CI expansion of the initial state actually contributing to q (in particular to $\langle \psi_{g,m} | z_1 + z_2 | \phi_s \rangle$) is a $1s3s$ configuration, whose weight is smaller for ψ_g than for ψ_m. Hence the peaks observed in the cross sections are more Lorentzian for photoionization of He($2\,{}^1S^e$).

We can also see in Table I that, in general $\rho_m^2 \gtrsim \rho_g^2$. This can be understood with the help of Eq. (6). As $\sigma_g^0 \simeq \sigma_m^0$, we can write

$$\frac{\rho_m^2}{\rho_g^2} \simeq \frac{\left[\sum_\nu \langle \psi_m | z_1 + z_2 | P\psi^{0-}_{\nu\mathcal{E}_s} \rangle \langle P\psi^{0-}_{\nu\mathcal{E}_s} | P\mathcal{H}Q | \phi_s \rangle\right]^2}{\left[\sum_\nu \langle \psi_g | z_1 + z_2 | P\psi^{0-}_{\nu\mathcal{E}_s} \rangle \langle P\psi^{0-}_{\nu\mathcal{E}_s} | P\mathcal{H}Q | \phi_s \rangle\right]^2} \gtrsim 1 , \tag{7}$$

where we have used Eqs. (2) and (3) and the fact that the largest partial widths (see paper I), and, therefore, the largest $\langle P\psi^{0-}_{\mu E} | P\mathcal{H}Q | \phi_s \rangle$ matrix elements are for the $2s\varepsilon p$, $2p\varepsilon s$, and $2p\varepsilon d$ channels. The maximum of the total cross section in the vicinity of a resonance is given by

$$\sigma^{\max} = \sigma^0[\rho^2(q^2+1)+1-\rho^2] . \tag{8}$$

Then, $\rho_m^2 > \rho_g^2$ together with $|q_m| > |q_g|$ imply that the resonance peaks are much more pronounced when helium is photoionized from the $2\,{}^1S^e$ state. The same holds, obviously, for the $n=2$ cross sections.

Finally, in order to compare with the available theoretical calculations of photoionization cross sections for metastable $2\,{}^1S^e$ helium, we have extended our results up to photon energies of 85 eV. In Fig. 3 we compare our σ_{2s} and σ_{2p} partial cross sections with those of Jacobs and Burke [6]. We have excluded from our results the region between 52 and 55 eV since our basis is not able to accurately reproduce the resonance structure in such a region. The general agreement for the σ_{2p} cross section is good. The σ_{2s} cross section is slightly higher than that of Jacobs and Burke, although both curves are almost parallel in most of the energy range considered in Fig. 3.

This work has been partially supported by the EEC twining program No. SCI*.0138.C(JR) and the DGICYT Project No. PB90-0213.

[1] P. R. Woodruff and J. A. R. Samson, Phys. Rev. Lett. **45**, 110 (1980); Phys. Rev. A **25**, 848 (1982); D. W. Lindle, T. A. Ferrett, U. Becker, P. H. Kobrin, C. M. Truesdale, H. G. Kerkhoff, and D. A. Shirley, *ibid.* **31**, 714 (1985); D. W. Lindle, T. A. Ferrett, P. A. Heimann, and D. A. Shirley, *ibid.* **36**, 2112 (1987); M. Zubek, G. C. King, P. M. Rutter, and F. H. Read, J. Phys. B **22**, 3411 (1989); M. Zubek, G. Dawber, R. I. Hall, L. Avaldi, K. Ellis, and G. C. King, *ibid.* **24**, L337 (1991); J. Jiménez-Mier, C. D. Caldwell, M. G. Fleming, and D. L. Ederer, Phys. Rev. A **44**, 5615 (1991).
[2] R. S. Van Dyck, Jr., C. E. Johnson, and H. A. Shugart, Phys. Rev. Lett. **25**, 1403 (1970).
[3] D. W. Norcross, J. Phys. B **4**, 652 (1971).
[4] H. Doyle, M. Oppenheimer, and A. Dalgarno, Phys. Rev. A **11**, 909 (1975).
[5] U. I. Safronova, V. S. Senashenko, and S. V. Khristenko, Opt. Spectrosc. **45**, 333 (1978).
[6] V. L. Jacobs and P. G. Burke, J. Phys. B **5**, 2272 (1972).
[7] K. L. Bell, A. E. Kingston, and I. R. Taylor, J. Phys. B **6**, 2271 (1973).
[8] A. Wague, Z. Phys. D **15**, 199 (1990).
[9] I. Sánchez and F. Martín, Phys. Rev. A **44**, 7318 (1991).
[10] C. L. Pekeris, Phys. Rev. **127**, 509 (1962).
[11] H. Feshbach, Ann. Phys. (N. Y.) **19**, 287 (1962); Y. Hahn, T. F. O'Malley, and L. Spruch, Phys. Rev. **128**, 932 (1962).
[12] F. Martín, O. Mó, A. Riera, and M. Yáñez, Europhys. Lett. **4**, 799 (1987); J. Chem. Phys. **87**, 6635 (1987).
[13] I. Sánchez and F. Martín, Phys. Rev. A **45**, 4468 (1992).
[14] U. Fano, Phys. Rev. **124**, 1866 (1961); U. Fano and J. W. Cooper, *ibid.* **137**, A1364 (1965).
[15] D. R. Herrick and O. Sinanoglu, Phys. Rev. A **11**, 97 (1975).